frontiers in Materials

ORIGINAL RESEARCH
published: 22 May 2020
doi: 10.3389/fmats.2020.00145

Crystal Structure, Infrared Spectra, and Microwave Dielectric Properties of $Ce_2(Zr_{0.94}Sn_{0.06})_3(MoO_4)_9$ Ceramics With Low Sintering Temperature

Huanrong Tian[1], *Xin Liu*[1], *Yaokang Yang*[1], *Haitao Wu*[1]* *and Zhiliang Zhang*[2]*

[1] School of Materials Science and Engineering, University of Jinan, Jinan, China, [2] State Key Laboratory of Biobased Material and Green Papermaking, Qilu University of Technology (Shandong Academy of Sciences), Jinan, China

OPEN ACCESS

Edited by:
Antonio Feteira,
Sheffield Hallam University,
United Kingdom

Reviewed by:
Kaixin Song,
Hangzhou Dianzi University, China
Raz Muhammad,
Abdul Wali Khan University
Mardan, Pakistan
Hadi Barzegar Bafrooei,
Hangzhou Dianzi University, China

***Correspondence:**
Haitao Wu
mse_wuht@ujn.edu.cn
Zhiliang Zhang
zhzhl@iccas.ac.cn

Specialty section:
This article was submitted to Ceramics and Glass, a section of the journal Frontiers in Materials

Received: 16 February 2020
Accepted: 24 April 2020
Published: 22 May 2020

Citation:
Tian H, Liu X, Yang Y, Wu H and Zhang Z (2020) Crystal Structure, Infrared Spectra, and Microwave Dielectric Properties of $Ce_2(Zr_{0.94}Sn_{0.06})_3(MoO_4)_9$ Ceramics With Low Sintering Temperature. Front. Mater. 7:145. doi: 10.3389/fmats.2020.00145

$Ce_2(Zr_{0.94}Sn_{0.06})_3(MoO_4)_9$ (CZSM) ceramics were synthesized via a traditional solid-state method. The effects of Sn-substitution on phase composition, microstructure, and microwave dielectric properties as a function of sintering temperature were discussed. The XRD results indicated that all the samples exhibited a single phase. The chemical bonds of CZSM ceramics were calculated based on P-V-L theory, which could be used to evaluate the relationship between structure and microwave dielectric properties. The tendency of dielectric constant was depended on the theoretical dielectric polarizability and bond ionicity. Moreover, the improvement of $Q{\cdot}f$ value was ascribed to the increase of packing fraction. The reduced τ_f value could be explained by decrease of the bond energy, enhanced the co-efficient of thermal expansion and increase of bond valence ($V_{Zr(Sn)}$). The complex permittivity values were obtained from infrared reflectivity spectra. The dielectric permittivity and loss were 10.92 and 3.08×10^{-4}, respectively, which agreed well with the measured value. Typically, the optimal microwave dielectric properties of $\varepsilon_r = 10.35$, $Q{\cdot}f = 59{,}660$ GHz (at 9.70 GHz), and $\tau_f = -7.52$ ppm/°C were achieved in CZSM ceramics sintered at 800°C for 6 h.

Keywords: $Ce_2(Zr_{0.94}Sn_{0.06})_3(MoO_4)_9$, low-temperature sintering, microwave dielectric properties, chemical bonds theory of complex crystals, infrared spectra

INTRODUCTION

Owing to the characteristics of light weight, low cost, and high performance, the microwave dielectric ceramics have been widely used as filters, waveguides, resonators, substrates, and waveguides (Cava, 2001; Reaney and Iddles, 2006; Li et al., 2018; Chen et al., 2019; Cheng et al., 2019; Wu et al., 2019). Currently, 5th generation mobile communication systems have received increasing attention (Zhou et al., 2017; Pang and Zhou, 2019; Bafrooei et al., 2020; Lin et al., 2020). To meet the microwave devices applied at millimeter wave, new materials and technologies are required. As a new ceramic fabrication technology, the low temperature co-firing ceramics (LTCC) technology have been intensively studied, it provide the platform for fabrication of three-dimensional ceramic modules (Yu et al., 2015; Sebastian et al., 2016; Guo et al., 2019; Hsiang et al., 2019; Song et al., 2020). Materials in this discipline require a low sintering temperature to co-fire with electrode material and suitable properties: a low dielectric constant (ε_r) to avoid the signal delay, a high quality factor

($Q{\cdot}f$) for better selectivity at higher frequencies and a near-zero temperature coefficient of resonant frequency (τ_f) for the frequency stability (Song et al., 2018; Lin et al., 2020). Therefore, it is essential to develop the microwave materials with low permittivity and high $Q{\cdot}f$ value.

Recently, Mo-based dielectric ceramics have been widely reported owing to low sintering temperature (<960°C) and good microwave dielectric properties (Choi et al., 2007; Pang et al., 2011; Surjith and Ratheesh, 2013; Zhang et al., 2015, 2019; Liu and Zuo, 2017, 2018; Tao et al., 2019; Xing et al., 2019; Zhang and Wu, 2019; Zheng et al., 2020). Among these excellent materials, the $Ce_2Zr_3(MoO_4)_9$ ceramic was regarded as candidate for LTCC materials applications due to low sintering temperature and near-zero τ_f value (Tao et al., 2019). However, the $Ce_2Zr_3(MoO_4)_9$ ceramics exhibited a higher dielectric losses, some strategies should be adopted in this paper. A large of studies for improving microwave dielectric properties have been carried out via Sn^{4+} ions substitution (Yang et al., 2009; Ma et al., 2013; Li et al., 2019). For instance, when x value increased from 0.0 to 0.6, the quality factor of $Ca(Sn_{1-x}Si_x)O_3$ (x = 0.5–1.0) ceramics increased from 16,000 to 63,000 GHz (Ma et al., 2013). The optimal microwave dielectric properties of $Mg_2(Ti_{0.8}Sn_{0.2})O_4$ ceramics with ε_r = 12.18, $Q{\cdot}f$ = 170,130 GHz, and τ_f = −53.1 ppm/°C (Li et al., 2019). Thus, Sn^{4+} ions substitution was taken to improve $Q{\cdot}f$ value of $Ce_2Zr_3(MoO_4)_9$ ceramics in this work. The $Ce_2(Zr_{0.94}Sn_{0.06})_3(MoO_4)_9$ (CZSM) ceramics were successfully prepared. The phase composition, sintering characteristics, microstructure, and dielectric properties of CZSM ceramics were investigated scientifically. Infrared reflectivity spectra (IR) and chemical bonds theory of complex crystals were adopted as useful tools to analyze the effect of intrinsic factor on microwave dielectric properties of CZSM ceramics.

EXPERIMENTAL

The reagent grade CeO_2 (99.9%, Macklin, China), ZrO_2 (99.99%, Macklin, China), SnO_2 (99.95%, Aladdin, China), and MoO_3 (99.95%, Aladdin, China) powders were used to fabricate CZSM ceramics by the traditional solid-state method. Based on the chemical formula, the raw materials were mixed by zirconia balls for 24 h with absolute ethanol as media. After drying at a temperature 80°C, the slurries were calcined at 700°C for 2 h. Then, the pre-sintered powders were crushed and re-milled for 24 h. Subsequently, 12 wt.% PVA added to the mixture, and the powders were pressed into pellets (10 mm in diameter and 6 mm in height). Finally, all the samples were sintered at 650–850°C for 6 h in air.

XRD was applied to examine the phase compositions of the sintered samples with Cu Kα radiation (D8 Advance, Bruker Co., Germany). The structure parameters and cell volume were obtained from refinement of XRD data using FullProf program. The microstructures of sintered samples were observed using SEM (FEI Co., United States) coupled with EDS. The ε_r value at microwave frequencies (13–15 GHz) and the $Q{\cdot}f$ value at microwave frequencies (9–11 GHz) were measured using the network analyzer (N5234A, Agilent Co., USA) (Hakki and Coleman, 1960; Courtney, 1970). The τ_f value was calculated using Equation (1):

$$\tau f = \frac{f_2 - f_1}{f_1(T_2 - T_1)} \times 10^6 (ppm/^\circ C) \quad (1)$$

where f_1 and f_2 are the resonant frequencies at the measuring temperatures T_1 (25°C) and T_2 (85°C), respectively. The apparent density was measured via the Archimedes method, and the theoretical density can be obtained through Equation (2).

$$\rho_{theory} = \frac{ZA}{V_c N_A} \quad (2)$$

where A, Z, and N_A are the atomic weight, number of atom in unit cell and volume of unit cell, respectively. The relative density was calculated by Equation (3):

$$\rho_{relative} = \frac{\rho_{apparent}}{\rho_{theory}} \times 100\% \quad (3)$$

RESULTS AND DISCUSSION

Figure 1 presented the XRD patterns of CZSM ceramics sintered between 650–850°C. It was observed that all of diffraction patterns match well with the $Pr_2Zr_3(MoO_4)_9$ (PDF#51-1851) phase, with no secondary phase detected. It indicated that all of sintered samples formed single phase solid solution, which belongs to trigonal system with R-3c (167) space group. To determinate its structure, refinement of the XRD data were conducted using FullProf program with Rietveld's method. The $Nd_2Zr_3(MoO_4)_9$ (ICSD File No. 92600) was used as starting

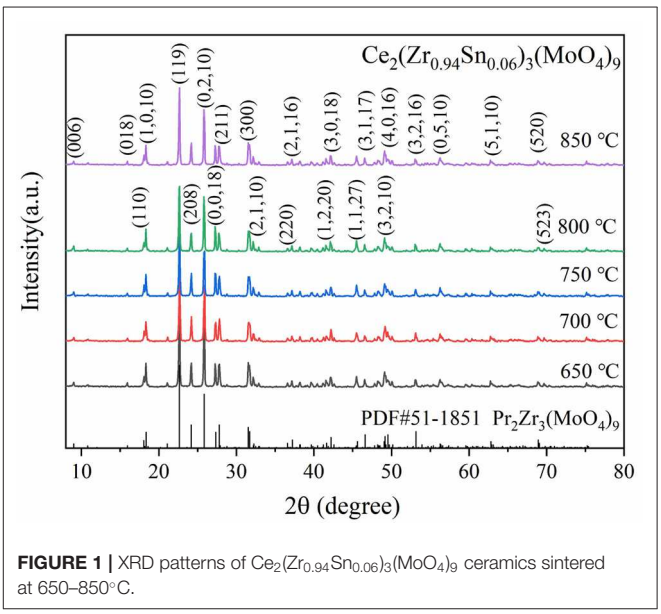

FIGURE 1 | XRD patterns of $Ce_2(Zr_{0.94}Sn_{0.06})_3(MoO_4)_9$ ceramics sintered at 650–850°C.

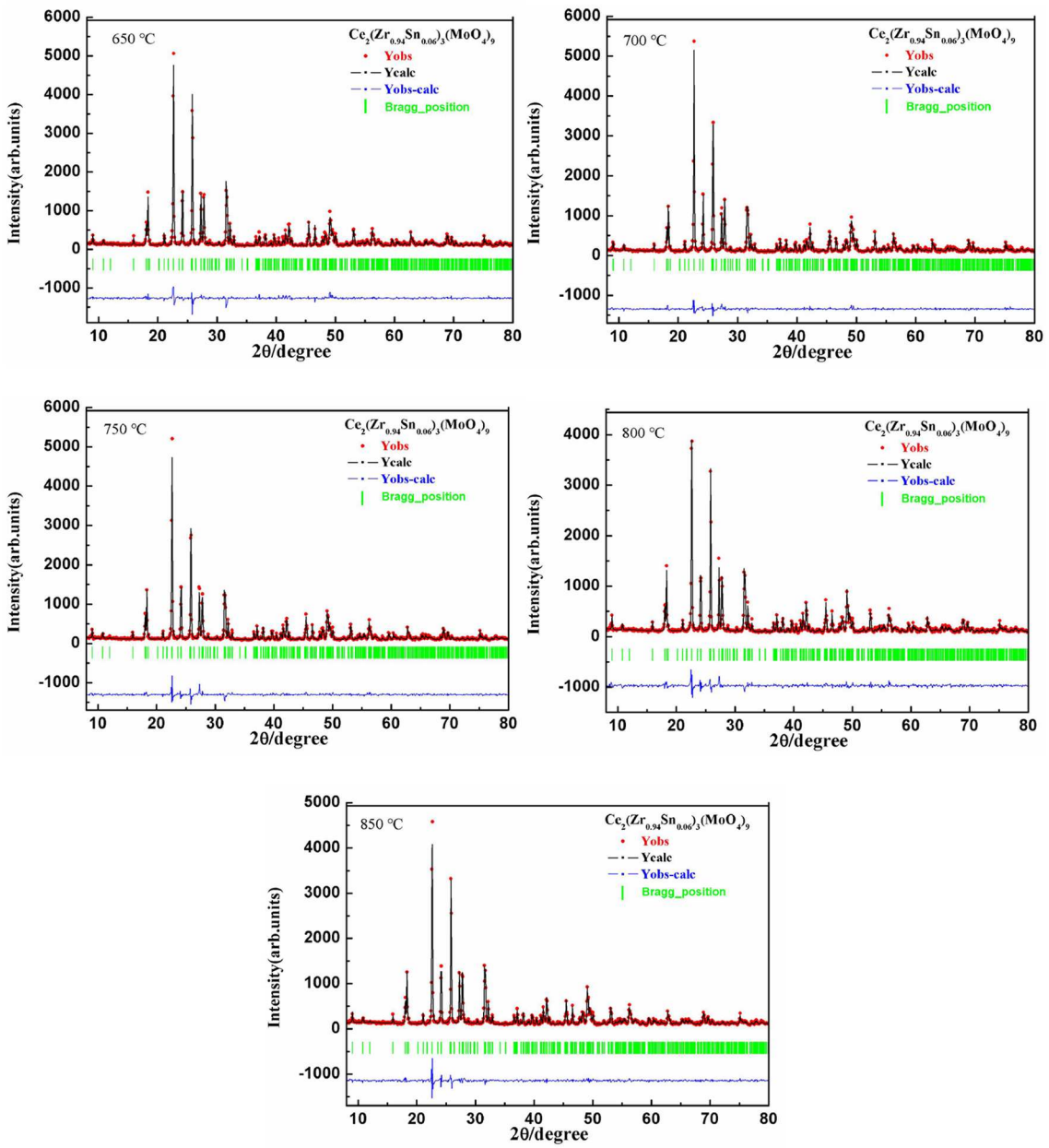

FIGURE 2 | Rietveld refinement of $Ce_2(Zr_{0.94}Sn_{0.06})_3(MoO_4)_9$ ceramics sintered at 650–850°C.

structural model. The refinement pattern of samples sintered at range of 650–850°C, as shown in **Figure 2**. The main crystallographic parameters and reliability factors of R_{wp}, R_p, and χ^2 for samples are summarized in **Table 1**. The R_{wp}, R_p, and χ^2 values were found to be in the range of 9.5–10.9, 7.2–8.6%, and 1.8–2.5, respectively. The value χ^2 were smaller to ensure the reliability of refinement. With the increasing sintering temperature, the a and b gradually increased from 9.8251 to 9.8269 Å, and c increased from 58.8278 to 58.8434 Å, which resulted in V_m increased from 4918.02 $Å^3$ at 650°C to 4921.14 $Å^3$ at 800°C. **Figure 3** presented crystal structure of CZSM ceramics. It can be seen that the Ce, Zr(1), Zr(2), Mo(1), and Mo(2) atoms are nearest neighbors to 9, 6, 6, 4, and 4 oxygen atoms, respectively. The [CeO_9] occupying the large cavities of the structure, the [CeO_9] and [ZrO_6] were connected by [MoO_4] at the structure.

Figure 4 illustrated the curves of the apparent and relative density of CZSM samples sintered at 650–850°C. The apparent densities increased from 3.50 g/cm^3 to the maximum value of 3.90 g/cm^3 with increasing sintering temperature. The relative density have same tendency as apparent density, a high relative density (>94%) was achieved at 750–850°C. Typical SEM images

TABLE 1 | The refinement parameters, theoretical densities and relative densities of $Ce_2(Zr_{0.94}Sn_{0.06})_3(MoO_4)_9$ ceramics fired at 650–800°C.

S.T.	$a = b$ (Å)	c (Å)	$\alpha = \beta$ (°)	γ (°)	V_m (Å^3)	R_p (%)	R_{wp} (%)	χ^2
650	9.825 (1)	58.827 (8)	90	120	4918.0 (2)	8.60	10.90	2.51
700	9.826 (6)	58.844 (3)	90	120	4920.8 (4)	7.24	9.55	1.85
750	9.826 (9)	58.840 (3)	90	120	4920.7 (4)	8.31	10.40	2.18
800	9.827 (7)	58.840 (3)	90	120	4921.7 (3)	8.35	10.90	2.36
850	9.827 (0)	58.843 (4)	90	120	4921.1 (4)	7.64	9.91	2.04

S.T., Sintering Temperature.
R_p, reliability factor of patterns.
R_{wp}, the reliability factor of weighted patterns.
χ^2, goodness of fit indicator = $(R_{wp}/R_{exp})^2$.

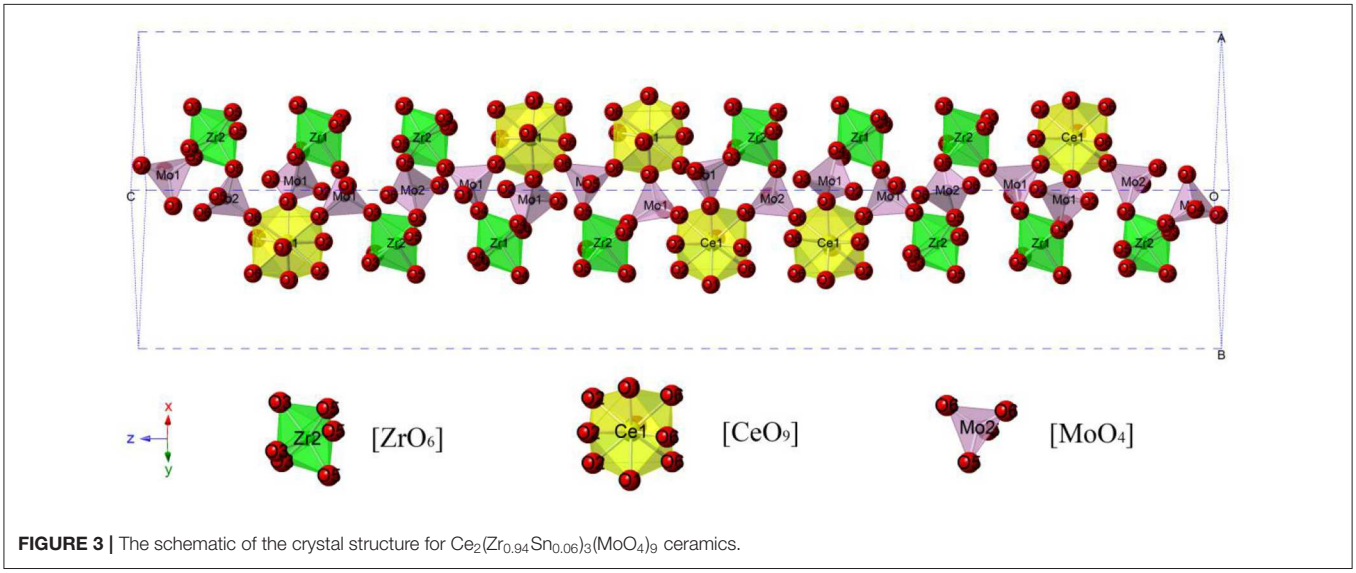

FIGURE 3 | The schematic of the crystal structure for $Ce_2(Zr_{0.94}Sn_{0.06})_3(MoO_4)_9$ ceramics.

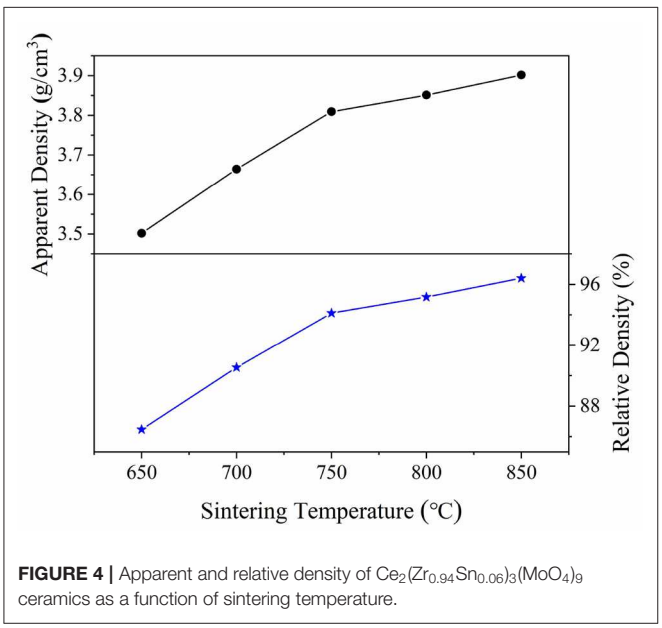

FIGURE 4 | Apparent and relative density of $Ce_2(Zr_{0.94}Sn_{0.06})_3(MoO_4)_9$ ceramics as a function of sintering temperature.

of CZSM ceramics sintered at different temperature were shown in **Figures 5A–E**. Grain boundaries were evident in all the samples, indicating that crystalline grains grew well in these samples. Moreover, the grain size increased from 1.93 to 3.19 μm and the pores gradually decreased with the increase of sintering temperature. The result of EDS about grain from samples sintered at 800°C was presented in **Figure 5F**. The ratio of Ce, Zr, Sn, Mo, and O atom were 3.93, 6.56, 0.34, 18.50, and 70.67%, respectively, which was corresponded to theoretical composition of CZSM ceramic.

The curves of microwave dielectric properties for CZSM samples were shown in **Figure 6**. The dielectric constant (ε_r) increased and reached maximum value of 10.47 as the temperature shifted from 650 to 750°C, and then kept stable with further increasing sintering temperature. In addition, the tendency of the ε_r value was corresponded to the density when sintering temperature at 650–800°C, suggesting that dielectric constant was closely related to the density in lower temperature. As we all know, apart from the extrinsic factors like density and phase composition, the ε_r also affected by the intrinsic factors such as polarizability and bond ionicity (Bi et al., 2018; Manan et al., 2018; Zhang et al., 2019). The XRD result suggesting the single phase ceramics was formed. Thus, the ε_r value of CZSM ceramics were mainly determined by polarizability and bond ionicity when the sample was compact. The theoretical dielectric polarizability ($\alpha_{theo.}$) and observed

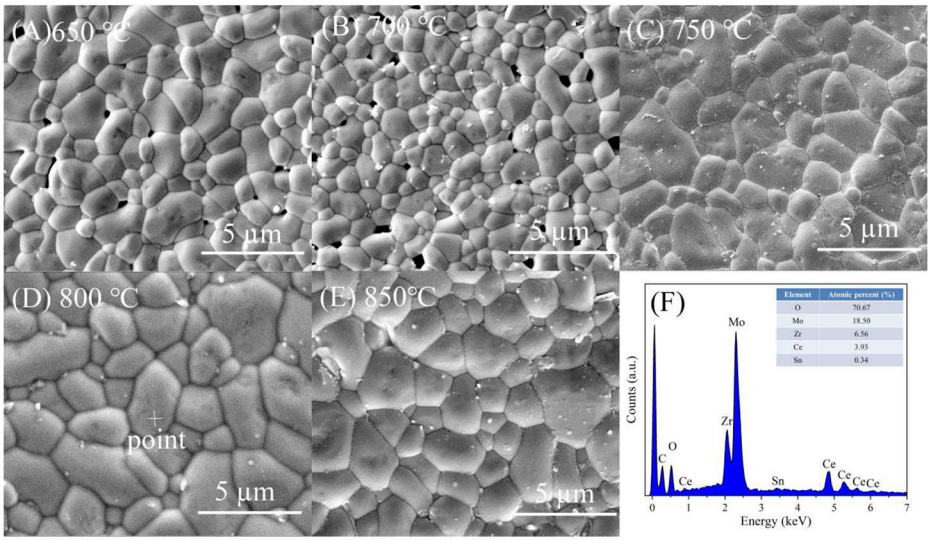

FIGURE 5 | Typical SEM micrographs of $Ce_2(Zr_{0.94}Sn_{0.06})_3(MoO_4)_9$ ceramics fired at **(A)** 650°C, **(B)** 700°C, **(C)** 750°C, **(D)** 800°C, **(E)** 850°C, and **(F)** EDS analysis about grain selected randomly from the sample sintered at 800°C.

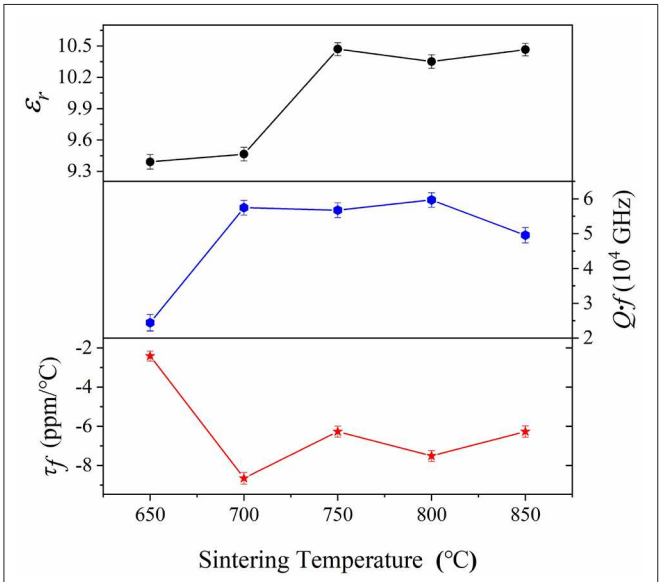

FIGURE 6 | Curves of microwave dielectric properties as a function of sintering temperature for $Ce_2(Zr_{0.94}Sn_{0.06})_3(MoO_4)_9$ ceramics in the temperature range from 650 to 850°C.

dielectric polarizability ($\alpha_{obs.}$) were calculated through Equations (4) and (5), respectively.

$$\alpha_{theo.}=\alpha(Ce_2(Zr_{0.94}Sn_{0.06})_3(MoO_4)_9) \quad (4)$$
$$= 2\alpha(Ce^{3+}) + 2.82\alpha(Zr^{4+}) + 0.18\alpha(Sn^{4+}) + 9\alpha(Mo^{6+}) + 36\alpha(O^{2+})$$

$$\alpha_{obs.} = \frac{1}{b} V_m \frac{\varepsilon - 1}{\varepsilon + 2} \quad (5)$$

where $\alpha(Ce^{3+}) = 6.15$ Å^3, $\alpha(Zr^{4+}) = 3.25$ Å^3, $\alpha(Sn^{4+}) = 2.83$ Å^3, $\alpha(O^{2+}) = 2.01$ Å^3 was reported by Shannon et al. and $\alpha(Mo^{6+}) = 3.28$ Å^3 is calculated by Choi et al. (Shannon, 1993; Choi et al., 2007). Moreover, V_m is the molar volume and b is a constant value ($4\pi/3$), respectively. The results were listed in **Table S1**. The $\alpha_{theo.}$ value (123.85 Å^3) lower than the $Ce_2Zr_3(MoO_4)_9$ ceramics (123.93 Å^3), which could be attributed to the smaller polarizability of Sn^{4+}:$\alpha(Sn^{4+}) = 2.83$ Å^3 < $\alpha(Zr^{4+}) = 3.25$ Å^3 (Tao et al., 2019). Besides, the tendency of ε_r value was similar to the $\alpha_{theo.}$ value and $\alpha_{obs.}$ value, indicating that the reduced ε_r value was strongly dependent on the decrease of polarizability.

Moreover, the quality factor($Q{\cdot}f$) increased from 24,410 to 59,660 GHz, and then declined slightly with further increasing sintering temperature, the maximum of the $Q{\cdot}f$ was 59,660 GHz at 800°C. In general, the dielectric losses are composed of intrinsic losses (lattice vibration) and extrinsic losses (grain size and impure phase). The grain size showed upward tendency with increasing sintering temperature, it was similar to the variation of $Q{\cdot}f$ value. Therefore, the increased grain size was important for improvement of the $Q{\cdot}f$ value (Yang et al., 2002, 2019; Ichinose and Shimada, 2006). In order to investigate the effect of the intrinsic factors, the packing fraction has been calculated by Equation (6).

$$packing\ fraction(\%) = \frac{volume\ of\ the\ atoms\ in\ the\ cell}{volume\ of\ unit\ cell} \times Z \quad (6)$$

where Z is the number of molecules per cell. Kim et al. reported the effective ionic size (Kim et al., 2010). The results indicated that the smaller ions size of Sn^{4+} (0.69 Å) substitution to Zr^{4+} (0.72 Å) lead to the higher packing fraction (47.84 > 47.74%). Thus, the improvement of $Q{\cdot}f$ value was ascribed to the increase of packing fraction. Furthermore, it suggested that the

Sn^{4+} ions substitution could improve the quality factor of $Ce_2Zr_3(MoO_4)_9$ ceramics.

The temperature co-efficient of resonant frequency (τ_f) of CZSM ceramics sintered at different temperatures from 650 to 850°C was shown in **Figure 6**. It can be seen that the saturation value of $\tau_f = -7.52$ ppm/°C was obtained when sintered at 800°C and kept stable at 700–850°C. The temperature coefficient of resonant frequency was associated with bond valence (Yoon et al., 2003; Cai et al., 2015). Therefore, the bond valence of $[Zr(Sn)O_6]$ octahedra can be obtained by Equations (7) and (8).

$$V_i = \sum_j v_{ij} \tag{7}$$

$$v_{ij} = \exp\left[\frac{(R_{ij} - d_{ij})}{b}\right] \tag{8}$$

where V_{ij} represent the sum of all the bond valences, R_{ij} is the bond valence parameter, d_{ij} is the length of the bond between atoms i and j, and b is an constant equal to 0.37. The results of bond valence were listed in **Table S1**. The bond valence ($V_{Zr(Sn)}$) increased from 8.92 to 9.17 with the Sn^{4+} substitution, and the τ_f value correlated to the change of bond valence ($V_{Zr(Sn)}$) (Tao et al., 2019). It indicated that the decline of τ_f value was related to the increase of bond valence ($V_{Zr(Sn)}$).

Figure 7 showed the microwave dielectric properties of Mo-based dielectric ceramics with low dielectric constant, and the parameters were summarized in **Table S2** (Choi et al., 2007; Pang et al., 2011; Surjith and Ratheesh, 2013; Zhang et al., 2015, 2019; Liu and Zuo, 2017, 2018; Tao et al., 2019; Xing et al., 2019; Zhang and Wu, 2019; Zheng et al., 2020). The CZSM ceramics possessed excellent microwave dielectric properties and low sintering temperature in this system. It suggests that they have potential for exploitation in LTCC technology. Certainly, it is necessary to study the relationship between structure and microwave dielectric properties. Thus, the bond ionicity, lattice energy, bond energy, and coefficients of thermal expansion were calculated to investigate the relationships between chemical bond and dielectric properties of the CZSM ceramic. Based on P-V-L theory, the complex crystals CZSM were decomposed into the sum of binary crystals as Equation (9) (Xue and Zhang, 1996; Wu et al., 1998; Yang et al., 2019):

$$\begin{aligned} &Ce_2(Zr_{0.94}Sn_{0.06})_3(MoO_4)_9 = Ce_2Zr/Sn(1)Zr/Sn(2)_2Mo(1)_6Mo(2)_3 \\ &O(1)_6O(2)_6O(3)_6O(4)_6O(5)_6O(6)_6 \\ &= Ce_{2/3}\,O(1)_3 + Ce_{2/3}\,O(2)_3 + Ce_{2/3}\,O(6)_3 \\ &+ Zr/Sn(1)O(4)_3 + Zr/Sn(2)O(3)_3 + Zr/Sn(2)O(5)_3 \\ &+ Mo(1)_{3/2}\,O(1)_3 + Mo(1)_{3/2}\,O(2)_3 + Mo(1)_{3/2}\,O(3)_3 \\ &+ Mo(1)_{3/2}\,O(4)_3 + Mo(2)_{3/2}\,O(5)_3 + Mo(2)_{3/2}\,O(6)_3 \end{aligned} \tag{9}$$

Equation (10) indicated that the dielectric constant can be predicted by bond ionicity (Batsanov, 1982).

$$\varepsilon_r = \frac{n^2 - 1}{1 - f_i} + 1 \tag{10}$$

where n is the refractive index. The bond ionicity were calculated using the Equations (11)–(13) (Xue and Zhang, 1996; Wu et al., 1998).

$$f_i^{\mu} = \frac{(C^{\mu})^2}{(E_g^{\mu})^2} = \frac{(C^{\mu})^2}{(E_h^{\mu})^2 + (C^{\mu})^2} \tag{11}$$

$$(E_h^{\mu})^2 = \frac{39.74}{(d^{\mu})^{2.48}} \tag{12}$$

$$C^{\mu} = 14.4 b^{\mu} exp(-k_s^{\mu} r_0^{\mu}) \left[\frac{(Z_A^{\mu})^*}{r_0^{\mu}} - (n/m)\frac{(Z_B^{\mu})^*}{r_0^{\mu}}\right] \tag{13}$$

$$k_s^{\mu} = (4k_F/\pi\alpha_B)^{1/2} \tag{14}$$

$$r_0^{\mu} = \frac{1}{2} d^{\mu} \tag{15}$$

where E_g^{μ} is the average energy gap, and it can be separated into homopolar E_h^{μ} and heteropolar c^{μ} parts. The $\exp(-k_s^{\mu} r_0^{\mu})$ is Thomas-Fermi prescreening factor, and it was calculated through Equations (14) and (15) (Levine, 1973). The f_i value of CZSM ceramics were shown in **Figure 8**, and the results were listed in **Table 2**. Decreasing sequence of f_i was f_i (Ce-O)> f_i (Zr/Sn-O)> f_i (Mo-O), the largest f_i value of 85.64% was obtained in Ce-O bond. Besides, the average of f_i (Ce-O) value decreased from 85.18 to 85.14% with the Sn^{4+} doped shifted from 0 to 0.06. The tendency of the ε_r value was consisted with the variation of f_i (Ce-O) value. It indicated that the reduced ε_r value was mainly dominated by the degressive bond ioniticy of Ce-O bond.

The dielectric loss can be control by the binding ability between cation and oxygen ion, high binding energy corresponds to low intrinsic loss. Thus, lattice energy of CZSM ceramics can be calculated by Equations (16)–(18) (Xue and Zhang, 1996; Wu et al., 1998).

$$U = \sum_{\mu} (U_{bi}^{\mu} + U_{bc}^{\mu}) \tag{16}$$

$$U_{bi}^{\mu} = 1270\frac{(m+n)Z_+^{\mu}Z_-^{\mu}}{d^{\mu}}(1 - \frac{0.4}{d^{\mu}})f_i^{\mu} \tag{17}$$

$$U_{bc}^{\mu} = 2100m\frac{(Z_+^{\mu})^{1.64}}{(d^{\mu})^{0.75}}f_c^{\mu} \tag{18}$$

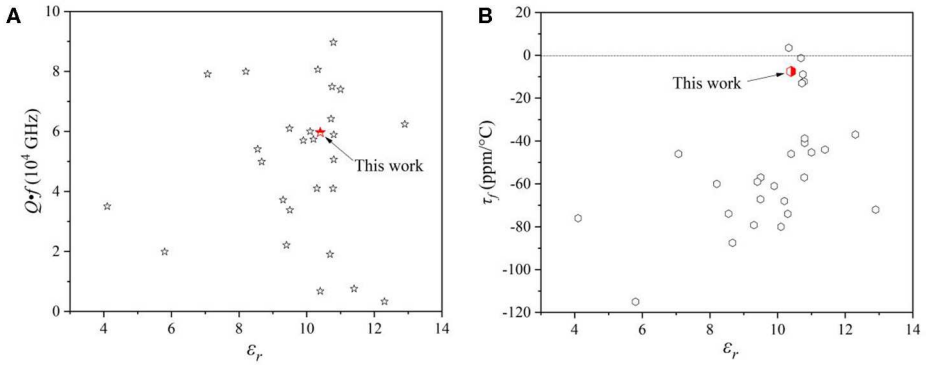

FIGURE 7 | (A) Quality factors ($Q{\cdot}f$) and **(B)** the temperature coefficient of resonant frequency (τ_f) of Mo-based microwave dielectric ceramics with a low dielectric constant.

TABLE 2 | Band ionicity f_i, lattice energy U, bond energy E, and coefficient of thermal expansion α of each bond for $Ce_2(Zr_{0.94}Sn_{0.06})_3(MoO_4)_9$ ceramic sintered at 800°C.

Bond type	Bond length(Å)	f_i (%)	U (KJ/mol)	α (10^{-6}/K)	E (KJ/mol)
Ce-O(1)^1 × 1	2.4084	84.74	3,403	9.7584	426.7504
Ce-O(1)^2 × 1	2.4091	84.74	3,402	9.7622	426.6264
Ce-O(1)^3 × 1	2.4094	84.74	3,401	9.7660	426.5733
Ce-O(2)^1 × 1	2.4595	85.03	3,343	9.9904	417.8840
Ce-O(2)^2 × 1	2.4597	85.03	3,343	9.9904	417.8500
Ce-O(2)^3 × 1	2.4602	85.03	3,342	9.9943	417.7651
Ce-O(6)^1 × 1	2.5766	85.64	3,214	10.5185	398.8922
Ce-O(6)^2 × 1	2.5767	85.64	3,214	10.5185	398.8768
Ce-O(6)^3 × 1	2.5772	85.64	3,214	10.5185	398.7994
Zr(Sn)1-O(4) × 6	2.0525	79.13	10,892	3.3839	502.1278
Zr(Sn)2-O(3)^1 × 1	2.1362	79.79	10,558	3.5912	482.4535
Zr(Sn)2-O(3)^2 × 1	2.1366	79.79	10,557	3.5918	482.3632
Zr(Sn)2-O(3)^3 × 1	2.1366	79.79	10,557	3.5918	482.3632
Zr(Sn)2-O(5)^1 × 1	1.9073	77.82	11,524	3.0245	540.3540
Zr(Sn)2-O(5)^2 × 1	1.9076	77.82	11,522	3.0256	540.2691
Zr(Sn)2-O(5)^3 × 1	1.9081	77.82	11,520	3.0267	540.1275
Mo(1)-O(1) × 1	1.8771	73.92	41,554	−0.2702	550.2277
Mo(1)-O(2) × 1	1.9894	74.82	39,853	−0.1465	519.1678
Mo(1)-O(3) × 1	1.7323	72.53	43,949	−0.4282	596.2202
Mo(1)-O(4) × 1	1.8027	73.24	42,754	−0.3516	572.9363
Mo(2)-O(5) × 2	1.8211	73.42	42,452	−0.3315	567.1475
Mo(2)-O(6) × 2	1.7552	72.77	43,554	−0.4033	588.4414
Ce-$O_{avg.}$	2.4819	85.14	-	10.0908	414.4464
Zr-$O_{avg.}$	2.0373	78.97	-	3.3463	506.7248
Mo-$O_{avg.}$	1.8193	73.36	-	−0.3333	568.7162

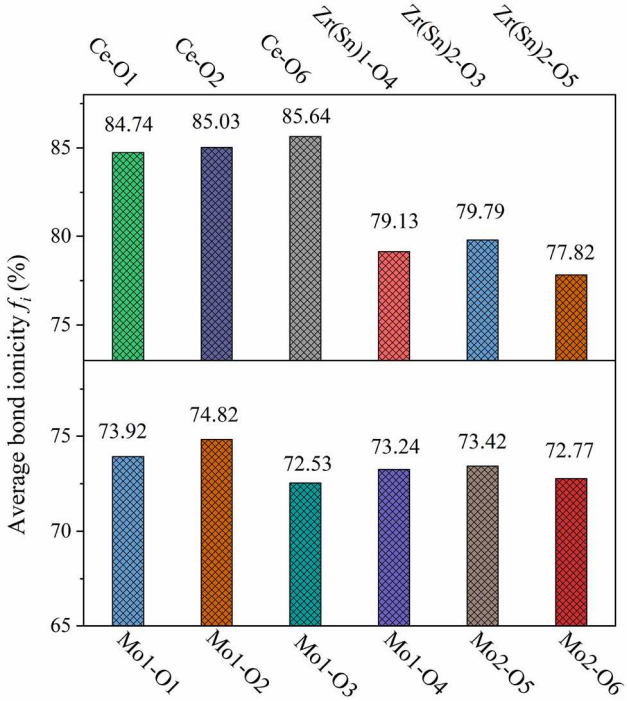

FIGURE 8 | Bond ionicity for $Ce_2(Zr_{0.94}Sn_{0.06})_3(MoO_4)_9$ ceramics sintered at 800°C.

where the lattice energy U_b^μ can be separated into covalent U_{bc}^μ and ionic U_{bt}^μ parts. According to **Figure 9**, the sequence of U (Mo-O)>U (Zr/Sn-O)>U (Ce-O) suggested that Mo-O bond play a vital role in enhancing the stability of ionic crystals.

What's more, the τ_f should be considered for realistic application of microwave dielectric ceramic. High bond energy could lead to a small absolute τ_f value. Hence, the bond energy can be obtained by Equations (19)–(21) (Sanderson, 1968, 1971, 1983):

$$E_b^\mu = t_c E_c^\mu + t_i E_i^\mu \tag{19}$$

$$E_i^\mu = \frac{33200}{d^\mu} \tag{20}$$

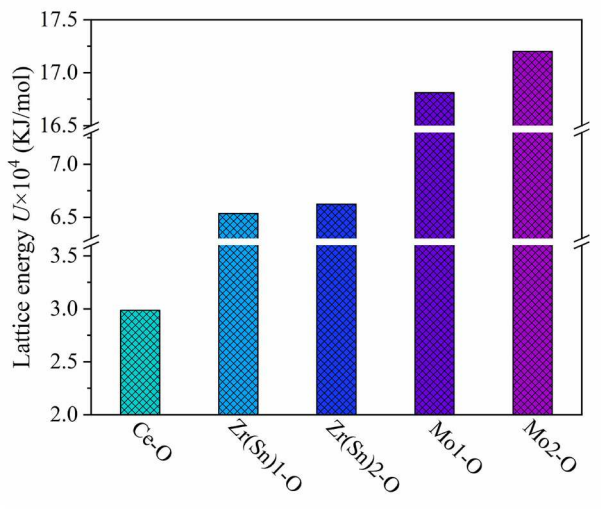

FIGURE 9 | Lattice energy for $Ce_2(Zr_{0.94}Sn_{0.06})_3(MoO_4)_9$ ceramics sintered at 800°C.

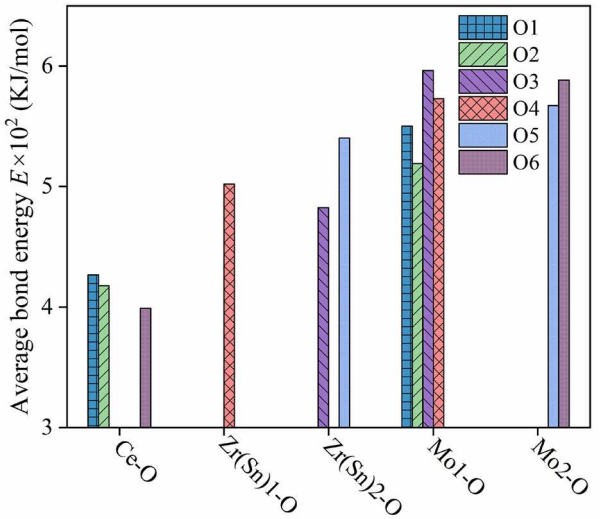

FIGURE 10 | Bond energy of different bond type for $Ce_2(Zr_{0.94}Sn_{0.06})_3(MoO_4)_9$ ceramics sintered at 800°C.

$$E_c^{\mu} = \frac{r_{cA} + r_{cB}}{d^{\mu}}(E_{A-A}E_{B-B})^{1/2} \quad (21)$$

where r_{cA} and r_{cB} are the covalent radii of atom A and atom B; t_i and t_c are ionic and covalent proportional coefficient of an individual bond μ. The bond energy E_{A-A} and E_{B-B} can be referred to handbook (Luo, 2007). What's more, S_A and S_B are the electronegativities of A and B atoms. **Figure 10** illustrated bond energy of different bond type for $Ce_2(Zr_{0.94}Sn_{0.06})_3(MoO_4)_9$ ceramics. The bond energy of Mo-O bond was larger than others, it suggested that Mo-O bond provided major contribution to the structural stability of CZSM ceramics. Compared with the $Ce_2Zr_3(MoO_4)_9$ ceramic, the bond energy of Mo-O bond declined from 574.8383 to 568.7162 KJ/mol. Meanwhile, the τ_f value was positively correlated with the change of bond energy (E_{Mo-O}). It suggested that the downward trend τ_f value could be explained by the decrease of bond energy (E_{Mo-O}).

The τ_f value was negatively related to the coefficients of thermal expansion, which can be obtained via Equation (22). Thus, the coefficients of thermal expansion were calculated based on P-V-L theory (Hakki and Coleman, 1960; Courtney, 1970; Xing et al., 2019).

$$\tau_f = -\left(\frac{\tau_\varepsilon}{2} + \alpha\right) \quad (22)$$

where τ_ε is temperature coefficient of the dielectric constant. The average values of Ce-O, Mo-O, and Zr/Sn-O bond were 10.0908 $\times$ 10^{-6} K^{-1}, -0.3333×10^{-6} K^{-1} and 3.3463×10^{-6} K^{-1}, respectively. In addition, The Mo-O bonds had a positive effect on τ_f value due to α_{Mo-O} value was negative. The α_{Mo-O} value increased from -0.3575×10^{-6} K^{-1} to -0.3333×10^{-6} K^{-1} because of the Sn^{4+} substitution for Zr^{4+}. The higher α_{Mo-O} value result in large absolute value. Hence, the reduced τ_f value was associated with enhanced the thermal expansion coefficient (α_{Mo-O}).

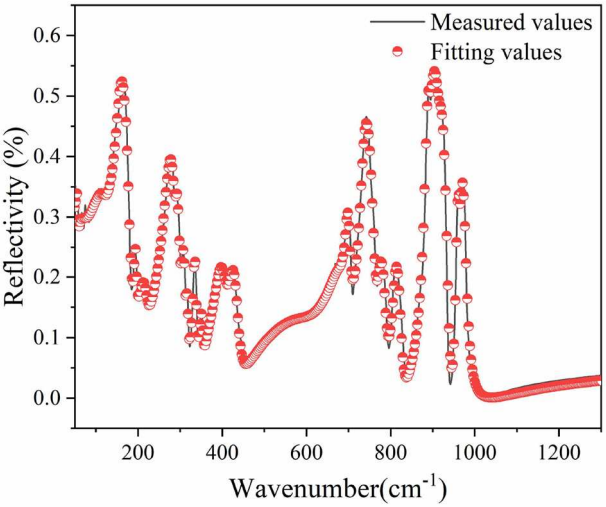

FIGURE 11 | Measured (black line) and fitted (red circle) infrared reflectivity spectra of $Ce_2(Zr_{0.94}Sn_{0.06})_3(MoO_4)_9$ ceramics sintered at 800°C.

IR reflectivity spectra of CZSM ceramics was exhibited in **Figure 11**. Based on the classical harmonic oscillator model, the infrared spectra were fitted with 24 internal modes, which were listed in **Table 3** (Petzelt and Kamba, 2003). ε^* (ω) (the complex dielectric permittivity) and R (ω) (the complex reflectivity) were calculated by Equations (23) and (24) (Wakino et al., 1986; Li et al., 2016; Tang et al., 2019; Guo et al., 2020).

TABLE 3 | Phonon parameters obtained from the fitting of the infrared spectra of $Ce_2(Zr_{0.94}Sn_{0.06})_3(MoO_4)_9$ ceramic sintered at 800°C.

Mode	$\varepsilon_\infty = 2.74$			
	ω_{oj}	ω_{pj}	γ_j	$\Delta\varepsilon_j$
1	56.63	31.15	4.545	0.3030
2	73.45	53.33	29.307	0.5270
3	117.86	137.00	39.089	1.3500
4	156.39	260.30	22.011	2.7700
5	193.49	56.51	6.926	0.0853
6	214.31	111.57	25.332	0.2710
7	273.66	261.46	24.191	0.9130
8	291.63	86.48	11.651	0.0879
9	306.77	82.12	10.579	0.0717
10	316.51	38.61	4.485	0.0149
11	334.32	96.06	7.964	0.0826
12	350.69	64.43	8.166	0.0338
13	397.64	211.24	32.055	0.2820
14	424.12	161.49	24.722	0.1450
15	589.11	376.94	175.040	0.4090
16	678.33	280.36	51.634	0.1710
17	697.73	203.30	12.768	0.0849
18	734.27	377.97	21.214	0.2650
19	774.94	168.59	21.378	0.0473
20	809.94	197.95	19.772	0.0597
21	884.55	333.41	10.980	0.1420
22	896.15	184.03	18.700	0.0422
23	914.91	81.92	21.151	0.0080
24	954.88	142.99	10.245	0.0224

Furthermore, the tan δ (dielectric loss tangent) can be obtained through Equation (25).

$$\varepsilon^*(\omega) = \varepsilon_\infty + \sum_{j=1}^{n} \frac{{\omega_{pj}}^2}{{\omega_{oj}}^2 - \omega^2 - j\gamma_j\omega} \tag{23}$$

$$R(\omega) = \left| \frac{1 - \sqrt{\varepsilon^*(\omega)}}{1 + \sqrt{\varepsilon^*(\omega)}} \right|^2 \tag{24}$$

$$tan\delta = \frac{\varepsilon''}{\varepsilon'} = \frac{\sum_{j=1}^{n} \Delta\varepsilon_j(\gamma_j\omega)/\omega_{oj}^2}{\varepsilon_\infty + \sum_{j=1}^{n} \Delta\varepsilon_j} \tag{25}$$

where ε_∞ is dielectric constant by electronic polarization, n is the number of transverse phonon modes, ω_{pj}, ω_{oj}, and γ_j are plasma frequency, transverse frequency and damping factors of the j-th Lorentz oscillator, respectively.

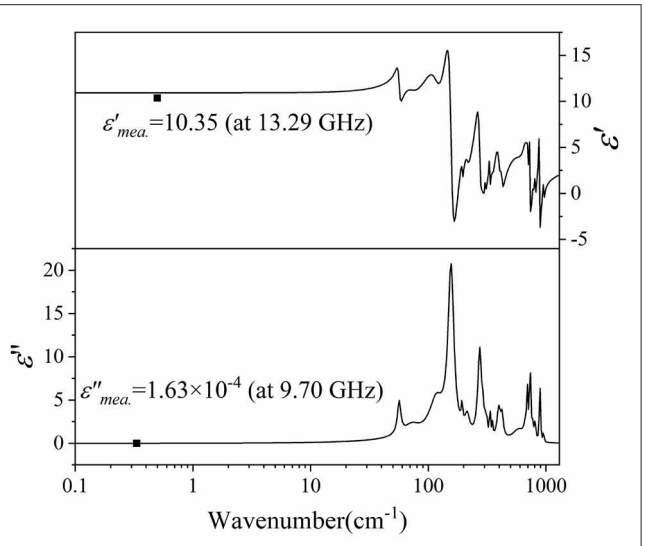

FIGURE 12 | The real and imaginary parts of the complex permittivity for $Ce_2(Zr_{0.94}Sn_{0.06})_3(MoO_4)_9$ ceramics sintered at 800°C (black points are measured value at microwave region).

Figure 12 presented the complex permittivity of CZSM ceramics sintered at 800°C. The extrapolated dielectric permittivity and loss were 10.92 and 3.08 × 10^{-4}, respectively. It can be seen that the calculated permittivity was slightly higher than the measured permittivity, the measured and calculated dielectric losses of CZSM ceramic were comparable with the same order of magnitudes. Therefore, the major dielectric contribution of the CZSM ceramics was in microwave region, and related to the absorptions of phonon oscillation.

CONCLUSION

$Ce_2(Zr_{0.94}Sn_{0.06})_3(MoO_4)_9$ (CZSM) microwave dielectric ceramics were successfully prepared. The XRD patterns demonstrated that all samples displayed a single phase. The SEM results indicated that nearly compact structure can be obtained sintered at 750–850°C. Subsequently, the dependence of microwave dielectric properties on intrinsic factors was evaluated based on P-V-L theory. The decrease of dielectric constant was mainly dominated by the decline of polarizability and bond ionicity of Ce-O bond. The improvement of quality factor was dependent on enhanced packing fraction. In addition, the reduced temperature coefficient of resonant frequency was related to the increase of thermal expansion coefficient and decrease of bond energy (E_{Mo-O}). The complex permittivity values were obtained by infrared spectra, which agreed well with the measured value. The CZSM ceramic sintered at 800°C exhibited an optimum microwave dielectric properties of $\varepsilon_r = 10.35$, $Q{\cdot}f = 59{,}660$ GHz (at 9.70 GHz) and $\tau_f = -7.52$ ppm/°C.

DATA AVAILABILITY STATEMENT

The raw data supporting the conclusions of this article will be made available by the authors, without undue reservation, to any qualified researcher.

AUTHOR CONTRIBUTIONS

HT: methodology, investigation, data curation, visualization, writing-original draft, and writing-review and editing. XL: investigation, validation, methodology, software and formal analysis. YY: software, validation, writing-review and editing. HW and ZZ: conceptualization, resources, writing-review and editing, project administration, supervision, and funding acquisition.

FUNDING

This work was supported by the National Natural Science Foundation of China (No. 51972143).

SUPPLEMENTARY MATERIAL

The Supplementary Material for this article can be found online at: https://www.frontiersin.org/articles/10.3389/fmats.2020.00145/full#supplementary-material

REFERENCES

Bafrooei, H. B., Liu, B., Su, W. T., and Song, K. X. (2020). $Ca_3MgSi_2O_8$: novel low-permittivity microwave dielectric ceramics for 5G application. *Mater. Lett.* 263:127248. doi: 10.1016/j.matlet.2019.127248

Batsanov, S. S. (1982). Dielectric methods of studying the chemical bond and the concept of electronegativity. *Russ. Chem. Rev.* 51, 684–697. doi: 10.1070/RC1982v051n07ABEH002900

Bi, J. X., Xing, C. F., Yang, C. H., and Wu, H. T. (2018). Phase composition, microstructure and microwave dielectric properties of rock salt structured Li_2ZrO_3-MgO ceramics. *J. Eur. Ceram. Soc.* 38, 3840–3846. doi: 10.1016/j.jeurceramsoc.2018.04.034

Cai, H. C., Li, L. X., Gao, Z. D., and Lv, X. S. (2015). A temperature stable microwave dielectric material $Ni_{0.35}Zn_{0.65}TiNb_2O_8$. *J. Mater. Sci. Mater. Electron.* 26, 998–1003. doi: 10.1007/s10854-014-2495-9

Cava, R. J. (2001). Dielectric materials for applications in microwave communications. *J. Mater. Chem.* 11, 54–62. doi: 10.1039/b003681l

Chen, X. L., Li, X., Zhou, H. F., Sun, J., Li, X. X., Yan, X., et al. (2019). Phase evolution, microstructure, electric properties of $(Ba_{1-x}Bi_{0.67x}Na_{0.33x})(Ti_{1-x}Bi_{0.33x}Sn_{0.67x})O_3$ ceramics. *J. Adv. Ceram.* 8, 427–437. doi: 10.1007/s40145-019-0326-4

Cheng, K., Li, C. C., Yin, C. Z., Tang, Y., Sun, Y. H., and Fang, L. (2019). Effects of Sr^{2+} substitution on the crystal structure, Raman spectra, bond valence and microwave dielectric properties of $Ba_{3-x}Sr_x(VO_4)_2$ solid solutions. *J. Eur. Ceram. Soc.* 39, 3738–3743. doi: 10.1016/j.jeurceramsoc.2019.05.030

Choi, G. K., Kim, J. R., Yoon, S. H., and Hong, K. S. (2007). Microwave dielectric properties of scheelite (A=Ca, Sr, Ba) and wolframite (A=Mg, Zn, Mn) $AMoO_4$ compounds. *J. Eur. Ceram. Soc.* 27, 3063–3067. doi: 10.1016/j.jeurceramsoc.2006.11.037

Courtney, W. E. (1970). Analysis and evaluation of a method of measuring the complex permittivity and permeability microwave insulators. *IEEE Trans. Microw. Theory Tech.* 18, 476–485. doi: 10.1109/TMTT.1970.1127271

Guo, H. H., Zhou, D., Liu, W. F., Pang, L. X., Wang, D. W., Su, J. Z., et al. (2020). Microwave dielectric properties of temperature-stable zircon-type (Bi, Ce)VO_4 solid solution ceramics. *J. Am. Ceram. Soc.* 103, 423–431. doi: 10.1111/jace.16759

Guo, H. H., Zhou, D., Pang, L. X., and Qi, Z. M. (2019). Microwave dielectric properties of low firing temperature stable scheelite structured (Ca, Bi)(Mo, V)O_4 solid solution ceramics for LTCC applications. *J. Eur. Ceram. Soc.* 39, 2365–2373. doi: 10.1016/j.jeurceramsoc.2019.02.010

Hakki, B. W., and Coleman, P. D. (1960). A dielectric resonator method of measuring inductive capacities in the millimeter range. *IRE Trans. Microw. Theory Tech.* 8, 402–410. doi: 10.1109/TMTT.1960.1124749

Hsiang, H. I., Chen, C. C., and Yang, S. Y. (2019). Microwave dielectric properties of $Ca_{0.7}Nd_{0.2}TiO_3$ ceramic-filled CaO-B_2O_3-SiO_2 glass for LTCC applications. *J. Adv. Ceram.* 8, 345–351. doi: 10.1007/s40145-019-0316-6

Ichinose, N., and Shimada, T. (2006). Effect of grain size and secondary phase on microwave dielectric properties of $Ba(Mg_{1/3}Ta_{2/3})O_3$ and $Ba([Mg,Zn]_{1/3}Ta_{2/3})O_3$ systems. *J. Eur. Ceram. Soc.* 26, 1755–1759. doi: 10.1016/j.jeurceramsoc.2005.09.032

Kim, E. S., Chun, B. S., Freer, R., and Cernik, R. J. (2010). Effects of packing fraction and bond valence on microwave dielectric properties of $A^{2+}B^{6+}O_4$ (A^{2+}: Ca, Pb, Ba; B^{6+}: Mo, W) ceramics. *J. Eur. Ceram. Soc.* 30, 1731–1736. doi: 10.1016/j.jeurceramsoc.2009.12.018

Levine, B. F. (1973). Bond susceptibilities and ionicities in complex crystal structures. *J. Chem. Phys.* 59, 1463–1486. doi: 10.1063/1.1680204

Li, C. C., Xiang, H. C., Xu, M. Y., Tang, Y., and Fang, L. (2018). Li_2AGeO_4 (A=Zn, Mg): two novel low-permittivity microwave dielectric ceramics with olivine structure. *J. Eur. Ceram. Soc.* 38, 1524–1528. doi: 10.1016/j.jeurceramsoc.2017.12.038

Li, H., Zhang, P. C., Yu, S. Q., Yang, H. Y., Tang, B., Li, F. H., et al. (2019). Structural dependence of microwave dielectric properties of spinel structured $Mg_2(Ti_{1-x}Sn_x)O_4$ solid solutions: crystal structure refinement, Raman spectra study and complex chemical bond theory. *Ceram. Int.* 45, 11639–11647. doi: 10.1016/j.ceramint.2019.03.037

Li, W. B., Zhou, D., Xi, H. H., Pang, L. X., and Yao, X. (2016). Structure, infrared reflectivity and microwave dielectric properties of $(Na_{0.5}La_{0.5})MoO_4$-$(Na_{0.5}Bi_{0.5})MoO_4$ ceramics. *J. Am. Ceram. Soc.* 99, 2083–2088. doi: 10.1111/jace.14175

Lin, Q. B., Song, K. X., Lin, B., Bafrooei, H. B., Zhou, D., Su, W. T., et al. (2020). Vibrational spectroscopy and microwave dielectric properties of $AY_2Si_3O_{10}$ (A=Sr, Ba) ceramics for 5G applications. *Ceram. Int.* 46, 1171–1177. doi: 10.1016/j.ceramint.2019.09.086

Liu, W. Q., and Zuo, R. Z. (2017). Low temperature fired $Ln_2Zr_3(MoO_4)_9$ (Ln=Sm, Nd) microwave dielectric ceramics. *Ceram. Int.* 43, 17229–17232. doi: 10.1016/j.ceramint.2017.09.083

Liu, W. Q., and Zuo, R. Z. (2018). A novel low-temperature firable $La_2Zr_3(MoO4)_9$ microwave dielectric ceramic. *J. Eur. Ceram. Soc.* 38, 339–342. doi: 10.1016/j.jeurceramsoc.2017.08.023

Luo, Y. R. (2007). *Comprehensive Handbook of Chemical Bond Energies*. Boca Raton: CRC Press. doi: 10.1201/9781420007282

Ma, Q., Wu, S. P., Jiang, C., and Li, J. H. (2013). Microwave dielectric properties of SnO_2-doped $CaSiO_3$ ceramics. *Ceram. Int.* 39, 2223–2229. doi: 10.1016/j.ceramint.2012.08.066

Manan, A., Ullah, Z., Ahmad, A. S., Ullah, A., Khan, D. F., Hussain, A., et al. (2018). Phase microstructure evaluation and microwave dielectric properties of (1-x)$Mg_{0.95}Ni_{0.05}Ti_{0.98}Zr_{0.02}O_3$-x$Ca_{0.6}La_{0.8/3}TiO_3$ ceramics. *J. Adv. Ceram.* 7, 72–78. doi: 10.1007/s40145-018-0258-4

Pang, L. X., Sun, G. B., and Zhou, D. (2011). $Ln_2Mo_3O_{12}$ (Ln=La, Nd): a novel group of low loss microwave dielectric ceramics with low sintering temperature. *Mater. Lett.* 65, 164–166. doi: 10.1016/j.matlet.2010.09.064

Pang, L. X., and Zhou, D. (2019). Modification of $NdNbO_4$ microwave dielectric ceramic by Bi substitutions. *J. Am. Ceram. Soc.* 102, 2278–2282. doi: 10.1111/jace.16290

Petzelt, J., and Kamba, S. (2003). Submillimetre and infrared response of microwave materials: extrapolation to microwave properties. *Mater. Chem. Phys.* 79, 175–180. doi: 10.1016/S0254-0584(02)00269-9

Reaney, I. M., and Iddles, D. (2006). Microwave dielectric ceramics for resonators and filters in mobile phone networks. *J. Am. Ceram. Soc.* 7, 2063–2072. doi: 10.1111/j.1551-2916.2006.01025.x

Sanderson, R. T. (1968). Multiple and single bond energies in inorganic molecules. *Inorg. Nucl. Chem. Lett.* 30, 375–393. doi: 10.1016/0022-1902(68)80464-6

Sanderson, R. T. (1971). *Chemical Bonds, Bond Energy*. New York, NY: Academic Press.

Sanderson, R. T. (1983). Electronegativity and bond energy. *J. Am. Chem. Soc.* 105, 2259–2261. doi: 10.1021/ja00346a026

Sebastian, M. T., Wang, H., and Jantunen, H. (2016). Low temperature co-fired ceramics with ultra-low sintering temperature: a review. *Curr. Opin. Solid. State. Mater. Sci.* 3, 151–170. doi: 10.1016/j.cossms.2016.02.004

Shannon, R. D. (1993). Dielectric polarizabilities of ions in oxides and fluorides. *J. Appl. Phys.* 73, 348–366. doi: 10.1063/1.353856

Song, J. B., Song, K. X., Wei, J. S., Lin, H. X., Wu, J., Xu, J. M., et al. (2018). Ionic occupation, structures, and microwave dielectric properties of $Y_3MgAl_3SiO_{12}$ garnet-type ceramics. *J. Am. Ceram. Soc.* 101, 244–251. doi: 10.1111/jace.15174

Song, X. Q., Lei, W., Zhou, Y. Y., Chen, T., Ta, S. W., and Fu, Z. X. (2020). Ultra-low fired fluoride composite microwave dielectric ceramics and their application for $BaCuSi_2O_6$-based LTCC. *J. Am. Ceram. Soc.* 103, 1140–1148. doi: 10.1111/jace.16795

Surjith, A., and Ratheesh, R. (2013). High Q ceramics in the $ACe_2(MoO_4)_4$ (A=Ba, Sr and Ca) system for LTCC applications. *J. Alloy. Compd.* 550, 169–172. doi: 10.1016/j.jallcom.2012.09.055

Tang, Y., Xu, M. Y., Duan, L., Chen, J. Q., Li, C. C., Xiang, H. C., et al. (2019). Structure, microwave dielectric properties, and infrared reflectivity spectrum of olivine type Ca_2GeO_4 ceramic. *J. Eur. Ceram. Soc.* 39, 2354–2359. doi: 10.1016/j.jeurceramsoc.2019.02.039

Tao, B. J., Xing, C. F., Wang, W. F., Wu, H. T., and Zhou, Y. Y. (2019). A novel $Ce_2Zr_3(MoO_4)_9$ microwave dielectric ceramic with ultra-low firing temperature. *Ceram. Int.* 45, 24675–24683. doi: 10.1016/j.ceramint.2019.08.206

Wakino, K., Murata, M., and Tamura, H. (1986). Far infrared reflection spectra of $Ba(Zn, Ta)O_3$-$BaZrO_3$ dielectric resonator material, *J. Am. Ceram. Soc.* 69, 34–37. doi: 10.1111/j.1151-2916.1986.tb04689.x

Wu, M. J., Zhang, Y. C., and Xiang, M. Q. (2019). Synthesis, characterization and dielectric properties of a novel temperature stable (1-x)$CoTiNb_2O_8$-x$ZnNb_2O_6$ ceramic. *J. Adv. Ceram.* 8, 228–237. doi: 10.1007/s40145-018-0308-y

Wu, Z. J., Meng, Q. B., and Zhang, S. Y. (1998). Semiempirical study on the valences of Cu and bond covalency in $Y_{1-x}Ca_xBa_2Cu_3O_{6+y}$. *Phys. Rev. B* 58, 958–962. doi: 10.1103/PhysRevB.58.958

Xing, C. F., Wu, B., Bao, J., and Wu, H. T., Zhou,Y. Y. (2019). Crystal structure, infrared spectra and microwave dielectric properties of a novel low-firing $Gd_2Zr_3(MoO_4)_9$ ceramic. *Ceram. Int.* 45, 22207–22214. doi: 10.1016/j.ceramint.2019.07.243

Xue, D. F., and Zhang, S. Y. (1996). Calculation of the non-linear optical coefficient of the $NdAl_3(BO_3)_4$ crystal. *J. Phys. Condens. Matter* 8, 1949–1956. doi: 10.1088/0953-8984/8/12/009

Yang, C. F., Tzou, W. C., Chung, H. H., Diao, C. C., and Huang, C. J. (2009). The microwave dielectric characteristics of $Ba(Ti_{4-x}Sn_x)O_9$ ceramics. *J. Alloy. Compd.* 477, 673–676. doi: 10.1016/j.jallcom.2008.10.081

Yang, H. C., Zhang, S. R., Yang, H. Y., Yuan, Y., and Li, E. Z. (2019). $Gd_2Zr_3(MoO_4)_9$ microwave dielectric ceramics with trigonal structure for LTCC application. *J. Am. Ceram. Soc.* 103, 1131–1139. doi: 10.1111/jace.16744

Yang, J. I., Nahm, S., Choi, C. H., Lee, H. J., and Park, H. M. (2002). Microstructure and microwave dielectric properties of $Ba(Zn_{1/3}Ta_{2/3})O_3$ ceramics with ZrO_2 addition. *J. Am. Ceram. Soc.* 85, 165–168. doi: 10.1111/j.1151-2916.2002.tb00060.x

Yoon, K. H., Kim, S. K., and Kim, E. S. (2003). Dependence of the octahedral bond valence on microwave dielectric properties of $Ca_{1-x}Sm_{2x/3}TiO_3$ ceramics. *Mater. Sci. Eng. B Adv.* 99, 112–115. doi: 10.1016/S0921-5107(02)00431-2

Yu, H. T., Liu, J. S., Zhang, W. L., and Zhang, S. R. (2015). Ultra-low sintering temperature ceramics for LTCC applications: a review. *J. Mater. Sci. Mater. Electron.* 12, 9414–9423. doi: 10.1007/s10854-015-3282-y

Zhang, G. Q., Wang, H., Guo, J., He, L., Wei, D. D., and Yuan, Q. B. (2015). Ultra-low sintering temperature microwave dielectric ceramics based on Na_2O-MoO_3 binary system. *J. Am. Ceram. Soc.* 98, 528–533. doi: 10.1111/jace.13297

Zhang, Y. H., Sun, J. J., Dai, N., Wu, Z. C., Wu, H. T., and Yang, C. H. (2019). Crystal structure, infrared spectra and microwave dielectric properties of novel extra low-temperature fired $Eu_2Zr_3(MoO_4)_9$ ceramics. *J. Eur. Ceram. Soc.* 39, 1127–1131. doi: 10.1016/j.jeurceramsoc.2018.12.042

Zhang, Y. H., and Wu, H. T. (2019). Crystal structure and microwave dielectric properties of $La_2(Zr_{1-x}Ti_x)_3(MoO_4)_9$ ($0 \leq x \leq 0.1$) ceramics. *J. Am. Ceram. Soc.* 102, 4092–4102. doi: 10.1111/jace.16268

Zheng, J. J., Xing, C. F., Yang, Y. K., Li, S. X., Wu, H. T., and Wang, Z. H. (2020). Structure, infrared reflectivity spectra and microwave dielectric properties of a low-firing microwave dielectric ceramic $Pr_2Zr_3(MoO_4)_9$. *J. Alloy. Compd.* 826:153893. doi: 10.1016/j.jallcom.2020.153893

Zhou, D., Pang, L. X., Wang, D. W., Li, C., Jin, B. B., and Reaney, I. M. (2017). High permittivity and low loss microwave dielectrics suitable for 5G resonators and low temperature co-fired ceramic architecture. *J. Mater. Chem. C* 5, 10094–10098. doi: 10.1039/C7TC03623J

Conflict of Interest: The authors declare that the research was conducted in the absence of any commercial or financial relationships that could be construed as a potential conflict of interest.